PHYSICAL REVIEW B VOLUME 15, NUMBER 5 1 MARCH 1977

Saturated superfluid-^{4}He film flow: Characteristic oscillations induced by persistent circulation*

Robert K. Galkiewicz and Robert B. Hallock†
Department of Physics and Astronomy, University of Massachusetts, Amherst, Massachusetts 01003
(Received 31 August 1976)

We report observations of characteristic reservoir oscillations induced by persistent circulation in saturated ^{4}He films for several different geometries. The shape of the oscillation structure appears to be in qualitative agreement with the predictions of Campbell. Within the constraints imposed by theoretical approximations and uncertainties in the experimental parameters, the quantitative agreement is satisfactory.

I. INTRODUCTION

Persistent currents have been known to exist in superfluid helium since 1961.[1] The early research into these currents involved bulk flow, and it was not until 1968[2] that such states were found to exist in relatively thin unsaturated films, and not until 1973[3] that research was initiated into persistent currents in thicker saturated films in open geometries.

Our initial measurements[4] were motivated by (i) the work of Hallock and Flint[5] who concluded that the damping of Atkins[6] oscillations between two reservoirs could be adequately accounted for by a mechanism first proposed by Robinson,[7] and hence was not due to processes within the film, and (ii) by the lack of observation of persistent currents in saturated films in the thick-film experiments of Wagner.[3] The experiments we report here were motivated primarily by Campbell,[8,9] who showed theoretically that reservoir oscillation anomalies[10-12] seen in various saturated film flow experiments could be explained by the presence of persistent film currents and who predicted characteristic oscillation structure for various geometries.

In this section we give a brief account of a number of previous persistent-current experiments. Section II is devoted to a brief review of oscillations between two reservoirs connected by saturated film along a single flow path. We then introduce Campbell's theory[8,9] for multiple flow paths and in Sec. III describe our apparatus and procedure. Some of our experimental observations are presented and interpreted in Sec. IV and we summarize our conclusions in Sec. V. Appendix A contains results and interpretations of some additional experiments performed on the creation and conservation of circulation in our apparatus.

A. Persistent bulk flow

The first experiment to observe persistent currents was that of Vinen[1] in 1961. In his experiment, a taut wire was set into transverse vibration and the circulation around it was deduced from the precession rate of the plane of vibration.[13] Vinen was able to observe a circulation of 1.96 h/m persist for a time of 100 min without detectable decay. In 1964 Bendt[14] and Depatie *et al.*[15] utilized very different techniques but arrived at the same conclusion: persistent currents existed in bulk superfluid HeII. After an experiment in 1964 by Reppy and Depatie[16] showed that the temperature-dependent angular momentum of a flow state scaled as the superfluid density, experimental attention shifted to the behavior of bulk flow through packed powders. Both Reppy[17] and Mehl and Zimmerman[18] developed gyroscopic techniques which employed packed powder to increase the critical velocity of the flow. These techniques, which actually measured the angular momentum of the persistent currents in a nondestructive manner, proved to be very sensitive and led to measurements of the temperature dependence of the superfluid fraction,[19] critical velocity,[20] and characteristic flow-velocity decay time[21] very near the lambda point.

In 1968 Van Alphen *et al.*[22] used yet another method to detect persistent currents. Following suggestions first presented by Sikora *et al.*,[23] the experimental apparatus consisted of two reservoirs connected by two paths of unequal length filled with packed powder. A persistent current could be established by drawing superfluid through both paths at the critical velocity thus generating a net circulation. By using a heater to block a short section of the shorter flow path, the kinetic energy of the persistent current could be trans-

formed into level oscillations of the two reservoirs connected to the flow paths.

The most recent method employed to detect persistent currents in packed powder was developed by Kojima *et al.*[24] who recognized that a persistent current would Doppler shift the speed of fourth sound in an annulus. Using this technique, these authors concluded there existed a vortex-free Landau state in rotating superfluid helium.

B. Unsaturated films

In a series of papers beginning in 1968, Reppy and co-workers[2,25,26] extended their investigations to unsaturated films. Utilizing their precise gyroscopic technique, Henkel *et al.*[2] were able to document the dependence of the onset of superfluid persistent currents on temperature and film thickness, and Chan *et al.*[25] demonstrated that persistent currents could exist in films only two atomic layers thick on a substrate preplated with neon.

Wang and Rudnick[27] have reported the lack of observation of persistent currents in unsaturated films. Their method consisted of measuring the time of flight of third sound pulses on a rotatable glass cylinder. If persistent currents were present then the flight time would be Doppler shifted. No Doppler shifting consistent with a persistent-current velocity greater than 1 cm/sec (the estimated uncertainty) was observed.

The null results of the Wang and Rudnick[27] experiment led Wagner[3] to conduct an experiment in which rotation of a polished copper cell was superimposed on a thermally induced film flow along the rotation axis. Wagner asserted that if persistent currents were present the critical flow rate for the thermally driven flow would depend on the angular velocity of the cell. No such dependence was observed for unsaturated or saturated films leading Wagner to conclude in agreement with Wang and Rudnick[27] that persistent flow characterized by high quantum numbers was very unstable.

C. Saturated films

In 1974, Verbeek *et al.*[28] observed persistent currents in saturated films using a method similar to that of van Alphen *et al.*[22] Two parallel flow paths were constructed from fine-glass capillary of 0.045-cm i.d. forming a 136-m-long loop closed by a 21-cm short section of packed powder. The kinetic energy of a persistent current flow in the loop could be blocked by raising the temperature of the packed powder, forcing the fluid into reservoirs where the resulting oscillations gave information regarding the direction and speed of the persistent current flow.

Later in 1974, Galkiewicz and Hallock[4] independently observed persistent currents in a flow loop consisting of relatively short (37 cm) and open (0.137-cm i.d.) stainless-steel tubing. This experiment was more comparable to the experiments of Wang and Rudnick[27] and Wagner,[3] and unlike all the remaining film experiments,[2,25,26,28] in that the flow path was everywhere (i) relatively open to vapor movement and (ii) free of packed powder.

Subsequently, Van Spronsen *et al.*[29] generated persistent currents in a geometry very similar to their previous one using rotational methods. This experiment indicated that there was nothing inherent in rotation itself to prevent the formation of persistent currents in relatively thick saturated films.

In 1974, Campbell[8] presented a theory of superfluid flow through multiply connected geometries that indicated the effects of persistent currents on the film oscillation between two reservoirs. Curious unexplained oscillation effects had been seen previously by a number of authors[5,10-12,30] but there had been no previous consideration of persistent currents in these experiments. In general these effects fell into two classes: (i) film oscillations which decayed with linear (rather than exponential) envelopes which abruply changed slope coincident with a dramatic change in oscillation frequency, and (ii) oscillations characterized by unusually large first-oscillation peaks relative to the remainder of the oscillation. As a result of our present understanding of the effects of persistent currents on film oscillations in various geometries,[8] it is now evident that the first clear experimental evidence for saturated film persistent currents was provided by the work of Hammel *et al.*[10]

II. FILM OSCILLATIONS

A. Simply connected geometries

Consider two reservoirs containing bulk HeII connected by a single film flow path located above the free surface of the liquid. If the equilibrium level of one reservoir is displaced relative to the other, the fluid will be accelerated over the flow path. Because in the isothermal limit the restoring force is proportional to the level difference, one would expect to observe undamped harmonic oscillations between the reservoirs. The frequency of these oscillations was first derived by Atkins[6] and is given by

$$\omega^2 = \frac{\rho_s}{\rho} g\left(\frac{1}{A_A} + \frac{1}{A_B}\right)\left(\int_A^B \frac{dl}{a(l)}\right)^{-1}, \tag{1}$$

where g is the gravitational acceleration, A_A and A_B are the cross-sectional areas of the respective

reservoirs, and the integral is taken along the film flow path of cross-sectional area $a(l)$. In fact it is generally observed that these oscillations are damped. The damping mechanism, as suggested by Robinson[7] for bulk flow, was first applied by Hoffer *et al.*[31] and Allen *et al.*[32] to film flow. Later, Hallock and Flint[5] carefully documented the quantitative validity of the Robinson[7] mechanism and showed that other proposed mechanisms[33-35] contributed a negligible amount to the overall damping. Robinson[7] damping is due to finite heat conduction between the two reservoirs. The flow of superfluid between the reservoirs results in temperature oscillations[36] which accompany the level oscillations. The resulting oscillating fountain pressure[37] opposes the film flow and leads to damping of the oscillations. This damping mechanism results in an exponential decay envelope (see Fig. 1).

Another more complex mode of dissipation for flow at high velocities can be seen in Fig. 1. Because the decay envelope does not extrapolate back to the displacement origin, it is evident that at some time between the level displacement and the first crossing of the new equilibrium level, energy has been lost from the system. It is generally believed that this dissipation is the result of thermal fluctuations[35,38] within the film, and while the identity of the specific excitation is still open to debate, experimental evidence indicates that this dissipation is a sharp function of velocity. Below the so-called "critical velocity" v_c the dissipation appears to be negligibly small, while above v_c the dissipation losses tend to balance any applied force to leave the velocity relatively unchanged (see Fig. 6 in Ref. 5). In the measurement shown in Fig. 1, the level displacement has been great

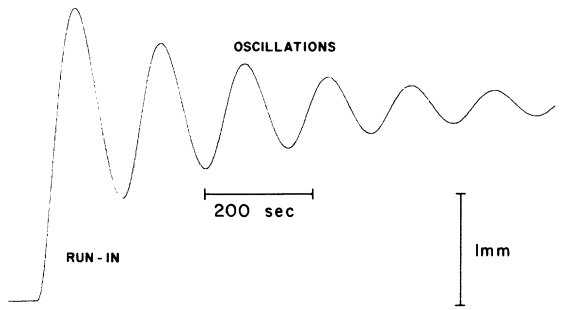

FIG. 1. Example of a measurement of the position of the free surface in reservoir A as a function of time during and after a change in the equilibrium level position. The run-in is characterized by high film flow velocity as the new equilibrium position is approached. The subsequent Atkins (Ref. 6) oscillations are exponentially damped consistent with expectations based on the work of Robinson (Ref. 7).

enough to accelerate the fluid to v_c and to dissipate energy. Note that no dissipation should be present after the first equilibrium zero crossing because the film always remains below v_c from that time on. That is, energy is lost from the flow primarily through dissipation during the "run-in" and primarily through Robinson[7] damping during the oscillations.

B. Multiply connected geometries

Following Campbell's derivation,[8] we now consider a system consisting of two reservoirs connected by a flow path, of effective area a_0 and effective length l_0, in series with two parallel (Fig. 2) paths of effective areas a_j and length l_j. The superfluid velocty v in each path obeys the equation

$$\frac{\partial \vec{v}}{\partial t} + \vec{\nabla}\left(\mu + \Omega + \frac{1}{2}\frac{\rho_s}{\rho}v^2\right) = \vec{f}(\vec{v}), \tag{2}$$

where μ is the chemical potential, Ω the Van der Waals potential, and $\vec{f}(\vec{v})$ describes the dissipation in the film as a function of velocity. If we integrate along the jth path from reservoir A to reservoir B under the assumption that the apparatus is bilaterally symmetric we have

$$\int_A^B \frac{d\vec{v}_j}{dt}\cdot d\hat{l}_j + \mu\Big|_A^B = \int_A^B \vec{f}(\vec{v}_j)\cdot d\hat{l}, \quad j=1,2. \tag{3}$$

After Campbell[8,9] we now take $\mu_B - \mu_A = gz - S\Delta T$ and $S\Delta T = -q\dot{z}$. Here g is the gravitation acceleration, z is the fluid level difference between the two reservoirs, S is the entropy of the liquid at temperature T, ΔT is the temperature difference between the two reservoirs, and q is a temperature- and geometry-dependent proportionality constant. With the further assumption of mass continuity we have that the product $v_j(l)a_j(l)$ is constant along any section of the flow path. Along the common section we will take that constant to be v_0a_0 and along the jth parallel path to be v_ja_j. We now have

$$\dot{v}_0 l_0 + \dot{v}_j l_j + gz + q\dot{z} = \int_A^B \vec{f}(\vec{v}_j)\cdot d\hat{l}_j, \quad j=1,2, \tag{4}$$

where

$$l_j = \int_A^B \frac{a_j dl_j}{a_j(l)}.$$

We finally include the general equation for mass continuity in our system

$$\rho A\dot{z} = \rho_s v_0 a_0 = \rho_s(a_1v_1 + a_2v_2). \tag{5}$$

Here A is the reduced reservoir surface area $A = A_AA_B/(A_A + A_B)$. After multiplying Eq. (4) by a_j/l_j, summing over j, and using Eq. (5) we have an equation of the form

$$\ddot{z} + 2b\dot{z} + \omega^2 z = D\,, \tag{6}$$

where

$$\omega^2 = \frac{g}{F}\sum_j{}'\left(\frac{a_j}{l_j}\right), \tag{7a}$$

$$b = \frac{q\omega^2}{2g}\,, \tag{7b}$$

$$D = \frac{1}{F}\sum_j{}'\left(\int_A^B \vec{f}(\vec{v}_j)\cdot d\hat{l}_j\right)\frac{a_j}{l_j}\,, \tag{7c}$$

$$F = \frac{\rho A}{\rho_s}\left[1 + \frac{l_0}{a_0}\sum_j{}'\left(\frac{a_j}{l_j}\right)\right], \tag{7d}$$

and $\sum_j'$ indicates a sum of $j=1$ to 2 *excluding* any path where $\dot{v}_j = 0$.

Equation (6) only admits solutions if the functional form for the dissipation, $\vec{f}(\vec{v})$, is known. However since $\vec{f}(\vec{v})$ is generally observed to be a sharp function of velocity one can gain much insight into the behavior of the system by assuming[8]

$$\vec{f}(\vec{v}_j) = 0 \quad \text{if } |v_j| < v_c\,, \quad j = 1,2\,; \tag{8a}$$

$$\frac{d\vec{v}_j}{dt} = 0 \quad \text{if } |v_j| = v_c\,, \quad j = 1,2\,. \tag{8b}$$

Equations (8a), (8b) model the behavior of no dissipation in film flowing at less than the critical velocity and no superfluid acceleration possible at greater-than-critical velocities. In addition it is easy to design a system such that $a_0 > a_1 + a_2$. If this is the case, we then expect $f(v_0) \equiv 0$ and Eq. (6) reduces to

$$\ddot{z} + 2b\dot{z} + \omega^2 z = 0\,, \tag{9}$$

which admits the solution

$$z(t) = z_0 e^{-bt}\sin(\omega' t + \phi)\,, \tag{10}$$

where $\omega' = (\omega^2 - b^2)^{1/2}$ and z_0 and ϕ are determined by the appropriate boundary conditions. Note that b and ω' change values every time a flow path starts or stops dissipating; our general solution may thus consist of many separate $z(t)$ joined into a smooth curve by requiring continuity in z and $\dot{z}$. Even with the approximation of Eqs. (8a) and (8b), the explicit appearance of e^{-bt} in Eq. (10) leads to transcendental boundary equations for the z and $\dot{z}$ continuity conditions. Consequently if the damping is small compared to the Atkins oscillation frequency it is useful to make the approximation $b = 0$. This approximation will allow us to solve for various oscillation parameters in closed form in Sec. IV.

III. APPARATUS AND PROCEDURE

A. Apparatus

The basic persistent current apparatus consisted of two coaxial capacitors[5] topped by copper tees (which had inside diameters of 0.795 cm in the horizontal sections, and 1.17 cm in the vertical sections) which connected long and short flow paths into a closed loop (see, Fig. 2). Placed in the bottom of each coaxial reservoir were a small manganin wire heater and a $\frac{1}{10}$ W carbon resistor thermometer. Capacitor A served as the reservoir level measuring detector and had a cross-sectional area of 2.13×10^{-2} cm^2 and a sensitivity of 1.08 cm/pF. Capacitor B, which could be coupled to a capillary fill line, had a cross-sectional area of 2.25×10^{-2} cm^2 and a sensitivity of 1.06 cm/pF. The capacitance of reservoir A was measured in a three terminal ac bridge configuration, which employed a GR-1615A capacitance bridge driven by a HP 651B test oscillator amplified by a McIntosh MC40 power amplifier. Off-null signals were amplified by a PAR HR-8 lock-in amplifier and recorded on an HP 7004A X-Y chart recorder operated in the time-Y mode.

The flow paths were made of stainless-steel tubing of 0.137-cm i.d. The length of the long flow path varied from 36.8 to 240 cm while the length of the short flow path varied from 1.16 to 1.27 cm depending on the specific experiment (Table I). These flow paths were wound with manganin wire (0.038-mm o.d.) at their midpoints over the span of roughly 0.25 cm. The purpose of the manganin heaters was to locally warm the flow path and so block the flow of superfluid film. As will be examined shortly, this technique[4] allowed us to check directly the magnitude and sense of any persistent current present in the loop. The wall thickness of the short flow path was reduced to

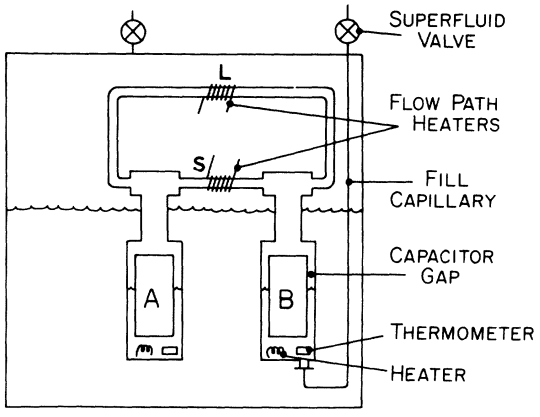

FIG. 2. Schematic diagram of the persistent current apparatus in the closed configuration. The reservoirs A and B are filled by use of the capillary as discussed in the text. The two film flow paths lie in approximately the same horizontal plane but are shown vertically separated here for clarity. The surrounding can is totally immersed in the main pumped Dewar bath (Ref. 5).

about 0.025 cm at the winding to facilitate heat transfer to the inner film. The height of the flow paths above the free surface was generally in the range of 6–7 cm and both flow paths were in the same horizontal plane to within ±1.0 cm. The detector assembly was partially immersed in a He bath contained in a sealed-brass can as shown in Fig. 2. The sealed can was immersed in the main pumped bath. The assembly could be run in two different configurations. The first configuration, which we term "closed" is that shown in Fig. 2. Here the detectors were filled by condensing purified He gas into a capillary immersed in the main bath over the can. This liquid then passed through a millipore filter,[39] a bellows-sealed superfluid valve,[40] and a capillary tubing (0.023-cm i.d.) before reaching the detectors. The detectors were usually filled at 1.5 K and subsequently the superfluid valve was shut to isolate the detector assembly. A second configuration, termed "open" was also used. This consisted of inserting a plunger into the can, and opening the detector assembly to the can bath by removing the fine capillary on reservoir B shown in Fig. 2. In the open configuration, the position of the free surface in the sealed can, and hence, in reservoir B could be changed up to 3 mm in approximately 1 sec by raising or lowering a plunger. The vibration of the apparatus caused by the manual operation of the plunger was not observable in reservoir A.

Two methods are generally available to initiate relative reservoir displacements in the closed configuration. One method consists of applying a dc voltage to one of the coaxial reservoir capacitors, thereby increasing the level in that reservoir by an amount proportional to the square of the applied voltage. Since in our apparatus the level displacement was limited by a voltage breakdown in the capacitor this technique was not used extensively. The other method consisted of utilizing the fountain effect by passing a current through one of the manganin wire heaters located in the base of the reservoirs. The heat input creates a chemical potential difference between the two reservoirs which acts to increase the equilibrium level of the hotter reservoir. In our apparatus this heat technique also creates a secondary bias film flow which moves to restore the atoms to the hotter reservoir that are lost through evaporation from the free surface. Unfortunately, for large enough heater powers this bias current visibly affected our ability to observe and create persistent currents. The closed configuration was consequently used exclusively for the study of small (0.05 cm or less) displacement phenomena and the open configuration used predominantly for larger displacements.

TABLE I. Flow path parameters and apparatus configuration for a number of experiments. The various parameters are defined in the text. Unless noted, the flow paths were stainless steel and the tees, copper. Exceptions are (a) stainless steel tees, (b) glass long flow path, and (c) short flow path removed.

Run	l_1 (cm)	l_2 (cm)	$1/l$	a	Configuration
I	1.92	37.5	19.5	1.04	closed
II[a]	2.38	240	101	1.00	closed
III	2.02	129	64.0	1.00	closed
IV	2.02	129	64.0	1.00	closed
V	2.02	129	64.0	1.00	open
VI[b]	2.01	128	63.0	0.74	closed
VII	1.91	129	68.0	0.85	open
VIII	1.91	129	68.0	0.85	open
IX	(c)	128	(c)	0	open

[a] Stainless-steel tees.
[b] Glass long flow path.
[c] Short flow path removed.

B. Procedure

We have employed two methods for producing persistent currents. The first, which will be called *trapping*, was used in Ref. 4. The second, termed *building-in*, can give information on the flow in each path without the use of the flow path heaters.[8]

1. Trapping

The data in Fig. 3 demonstrate how persistent currents are generated by trapping. At the beginning of the trace, an oscillation takes place through the long flow path alone since the short-flow-path heater (S) is on. At position (1) heater S is turned off, allowing fluid to flow through the short flow path and a persistent current is trapped in the loop. To obtain the most efficient energy transfer

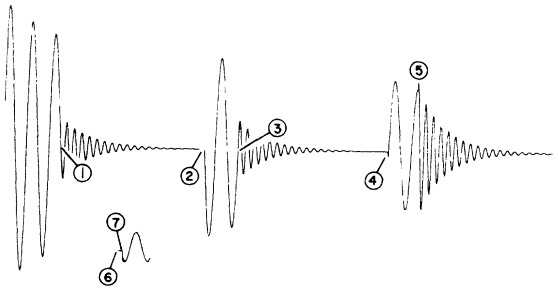

FIG. 3. Typical trapping of a persistent current. The low-frequency oscillations take place with the short-flow-path heater S on. A persistent current is trapped at (1) by shutting the heater S off, and observed at (2) by turning the heater on again. The complete sequence depicted here is described in more detail in the text (see also Ref. 4).

from oscillation to persistent current, the heater S should be turned off when the difference in the helium levels between the two reservoirs is zero. This is because the velocity in the long flow path is at a maximum at the zero crossing and the reservoir levels are in equilibrium. The oscillations after (1) are primarily due to the momentum of the fluid in the stand pipes connecting the coaxial capacitors to the tees. After a time τ when the oscillations have died out, heater S is turned on, redirecting the flow into a reservoir where the kinetic energy which had been trapped in the circulating persistent current is transferred into potential energy and subsequent level oscillations. This is shown at event (2). Event (3) represents the trapping and documentation (4) of a smaller magnitude persistent current travelling in the opposite sense of (1)–(2). At (5) the heater is switched off at an oscillation peak. At this point the velocity is zero in the long flow path and remains basically so while the reservoir levels equilibrate through the short flow path. The recording is continued at (6) and the oscillation at (7) represents a state-of-zero or near-zero persistent current and corresponds to the signature of the heater S alone. It should be noted that the size of the oscillation after (2) is observed to be independent of τ for times as large as 10 h. This suggests that to within our experimental uncertainty ($\approx$2%) the magnitude of the trapped kinetic energy is independent of τ for 1 min $\lesssim \tau \lesssim$ 10 h.[41] If one assumes these circulating currents to be metastable with a decay governed by fluctuation processes,[35] so that the film velocity decays logarithmically in time and further assumes that this decay continues for *all time*, this observation suggests a lower limit of the lifetime of these circulating film currents substantially in excess of the assumed present age of the universe. Thus, we are justified in terming these currents persistent.

The heater power used to interrupt the flow in the short flow path was determined at each temperature by plotting the decay constant governing the oscillation envelope as a function of heater power. For little or no applied power one sees the decay constant (α) and frequency (ω) characteristic of film flow through both flow paths. As the power is increased, partially blocking the short flow path, the damping increases until as the flow path becomes fully blocked the decay constant dramatically decreases to a constant value. Meanwhile the frequency drops and then rises to a value characteristic of flow through the long flow path as the short flow path becomes blocked. Both the decay constant and the frequency saturate at their long-flow-path values, and become insensitive to further increases in heater power. The behavior near the saturation region is illustrated in Fig. 4 where the heater operation point is chosen (5–10)% above the minimum saturation power to insure reproducibility. Since the heater is wrapped on the outside of the stainless-steel tubing only a fraction of the applied power reaches the inner film flow surface.

In experiments employing an open configuration and a different long flow path from that used for Fig. 4 we have found that the frequency obtained in the saturation region is within a few percent of that observed in a subsequent experiment with the short flow path removed. When the decay constants are compared, however, a 35% increase is observed for the run employing heater S over the run without the short flow path. This difference is not totally unexpected since the heater S significantly perturbs the temperature of the closed detector relative to the detector directly tied to the

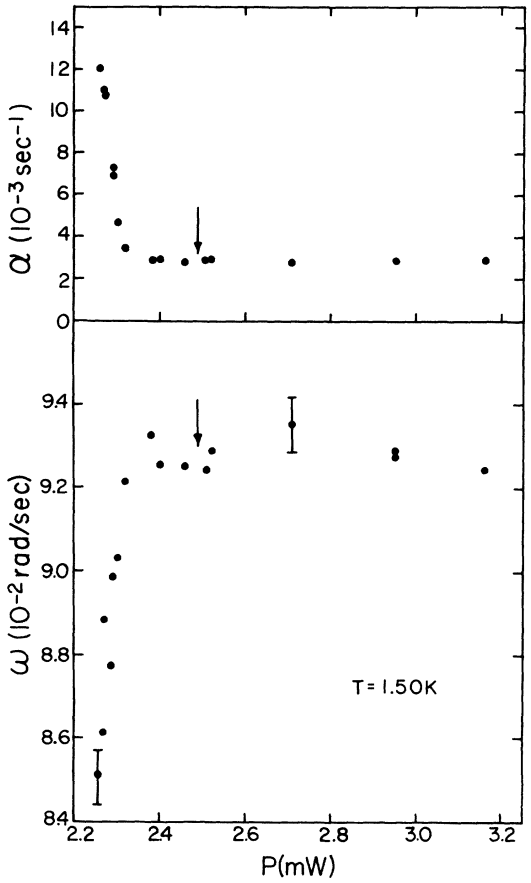

FIG. 4. Oscillation envelope decay constant and oscillation frequency as a function of total power applied to the short-flow-path heater S. The arrows represent the operating power at this particular temperature. Typical error bars for the frequency are indicated; error bars for the decay constant are smaller than the symbols. Note the difference in the range of the two vertical scales.

bath.

Once the heater power was selected at each temperature a study was made of the characteristics of the heater operation. Referring back to Fig. 3 one can see that corresponding to any given persistent current there exist a characteristic input and output oscillation. A graph of the peak-to-peak output oscillation amplitude $z_{pp,out}$ versus the peak-to-peak input amplitude $z_{pp,in}$ can indicate the existence of any heater-induced complications or asymmetries. Two such plots of $z_{pp,out}$ vs $z_{pp,in}$ are shown in Figs. 5 and 6. In both graphs the schematic sine curves indicate the sense of the persistent current. The inset indicates the heater "signature" corresponding to zero persistent current (refer to point 7 on Fig. 3).

The data shown in Fig. 5 are taken from an experiment employing a closed configuration; the inset shows that the heater causes only a slight perturbation of the system. There is basically no difference between the equilibrium level with S on or with S off so from Eq. (5) (mass continuity) we have that

$$v_{2\rho} \propto \dot{z}_{in} \quad (S \text{ switched off}); \tag{11a}$$

$$v_{2\rho} \propto \dot{z}_{out} \quad (S \text{ switched on}). \tag{11b}$$

Here $v_{2\rho}$ represents the persistent current velocity and $\dot{z}_{in}$ and $\dot{z}_{out}$ represent the reservoir fill rates

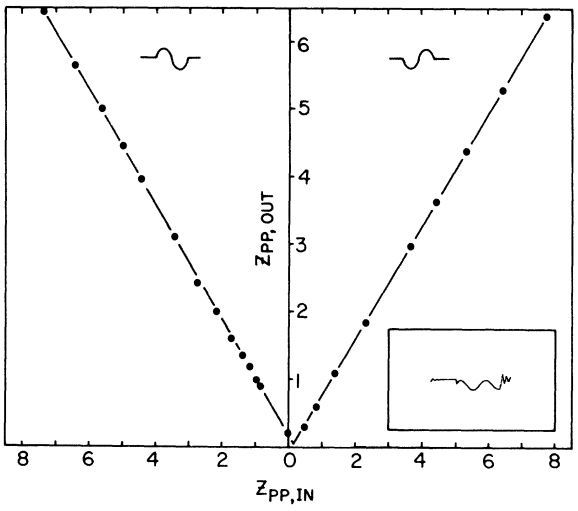

FIG. 5. Peak-to-peak output oscillation amplitude $z_{pp,out}$ vs the peak-to-peak input amplitude $z_{pp,in}$. The schematic sine curves in the upper portion of the figure show the sense of the oscillation. The inset shows the level in reservoir A vs time and displays the effect of operating the heater S with no persistent current in the apparatus. These data were obtained in a closed geometry (Fig. 2) at $T = 1.50$ K with $l_1/l_2 = \frac{1}{64}$ and $a_1/a_2 = 1$. One amplitude unit represents a 121-μm displacement in reservoir A for both the graph and the inset.

just before S is switched off and just after S is switched on during a trapping event. For a damped harmonic oscillator

$$\dot{z}_{in,(out)} = \beta \omega_2 z_{pp,in,(out)}, \tag{12}$$

where ω_2 is the frequency of oscillation while S is on and the constant β compensates for damping effects. If Eqs. (11a) and (11b) hold, we then expect that

$$z_{pp,out} = e z_{pp,in}, \tag{13}$$

where e is a proportionality constant that functionally represents the efficiency of the heater trapping sequence. This type of behavior is observed in Fig. 5 with $e = 0.84 \pm 0.01$.

An example of similar measurements made in an open configuration is shown in Fig. 6. These data were taken in a somewhat different manner due to the large heater offset visible in the inset. We believe this offset comes about in the following way. The existence of a heat input at S tends to draw superfluid out of the reservoirs and return vapor by condensation. Both of these effects tend to raise the temperature of the two reservoirs relative to the surrounding bath due to the finite thermal conductivity of the actual detector assemblies.[5] When the system is in the closed configuration this effect is minimized due to the general bilateral symmetry of our apparatus about S. This is apparent in Fig. 5 where the very minor offset is most probably due to slight asymmetries in the system. In employing an open system one breaks the symmetry by coupling the nonmeasuring reservori (B) to the surrounding bath both in temperature and free surface level. Consequently when S is applied, the temperature in reservoir A will

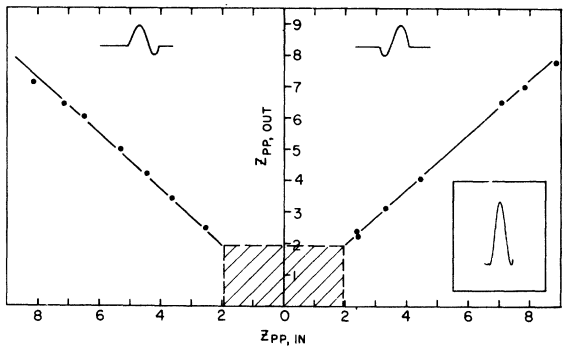

FIG. 6. Peak-to-peak oscillation amplitude vs the peak-to-peak input amplitude for the open geometry at $T = 1.30$ K. In this case $l_1/l_2 = \frac{1}{68}$ and $a_1/a_2 = 0.85$. Again the inset shows the level in reservoir A vs time after operating heater S with no persistent current in the apparatus. The effect is larger here than in case of the symmetric geometry. One amplitude unit represents 171-μm displacement in reservoir A.

rise relative to that in B creating a chemical potential difference between the two reservoirs. Superfluid will then be accelerated through the long low path as the system restores equilibrium by creating a pressure head (the heater offset) and, oscillations will occur (in the manner described in Sec. II A) between the two reservoirs about the new equilibrium level in A.

Because the heater offset shown in Fig. 6 was comparable to the minimum height needed to accelerate the fluid in the short flow path to v_c, the $S=0$ equilibrium level crossings were chosen as the heater on/off points instead of the heater-on equilibrium level (i.e., the center of the sine curve). In this way any dissipation was minimized at the insertion of a persistent current. Under this procedure, the analysis proceeds as before except that

$$\dot{z}_{\text{in,(out)}} = \beta\omega_2 \left(\tfrac{1}{4} z^2_{\text{pp,in,(out)}} - z_0^2\right)^{1/2}, \tag{14}$$

where z_0 represents the heater-induced level difference. Equation (13) then becomes

$$z_{\text{pp,out}} = 2z_0\left[1 - e^2 + (e z_{\text{pp,in}}/2z_0)^2\right]^{1/2}, \tag{15}$$

where e once again represents the trapping efficiency and we take $\dot{z}_{\text{pp,in}} \geq 2z_0$. This type of behavior is observed in Fig. 6 where $e = 0.90 \pm 0.01$ represents the indicated lines through the data points. The shaded region represents the region excluded due to the offset (i.e., $2z_0 = 1.9$ units). In this analysis the persistent current velocity scales as

$$v_{2p} \propto \left(z^2_{\text{pp,out}} - 4z_0^2\right)^{1/2}. \tag{16}$$

2. *Building in*

Campbell's theory[8] predicts that a persistent circulation can be induced without the use of a heater, and that the presence of the persistent current will be signaled by an anomalous characteristic initial peak in the oscillation structure. This anomalous peak, as shown in Fig. 7, can be generated in the apparatus of Fig. 2 in the following manner. First any circulation in the flow loop is reduced to a negligible amount by use of the heater S as described previously. Then the fluid equilibrium levels are displaced (by the use of the reservoir heater or plunger depending on the experimental configuration) so as to induce superfluid film flow through both paths toward reservoir A. If the level change is large enough, the fluid in the short flow path is quickly accelerated to its critical velocity v_c and dissipation occurs. The fluid in the long flow path comprises a larger effective mass and so takes longer to accelerate. Consequently at α in Fig. 7 the velocity in the short path v_1 is v_c while that in the long path v_2 is some fraction of v_c or for large enough level displacements v_c. Because of the inertia of the fluid in the flow paths, reservoir A overfills and the restoring force reverses direction. The fluid in the short path slows and then reverses direction tending to empty A, while the fluid in the long path only slows, filling A at a decreasing rate. At point β the net fill rate is zero, indicating that the reservoir is being emptied as fast as it is being filled. From shortly after β until point γ, the fluid in the short path dissipates energy at critical velocity while that in the long path continues to slow but still does not reverse direction. After γ there is no longer an amplitude-pressure head large enough to accelerate the fluid to v_c and thus no dissipation in the film. The peak $\alpha\beta\gamma$ is then anomalously large compared to the oscillations immediately following because energy has been lost in the flow somewhere in the segment $\beta\gamma$. Also, because the fluid in the long path has not been stopped but only slowed, a net circulation is created in a counterclockwise sense in the flow loop in Fig. 2. The process has built in a persistent current. The shape of the anomalous peak is determined both by the geometry of the flow paths and by the velocity in the long path at α. In Sec. IV we shall present detailed descriptions of the velocity dependence for various geometries.

IV. OBSERVATIONS

Consider now the apparatus in the open configuration with the capillary removed and a plunger

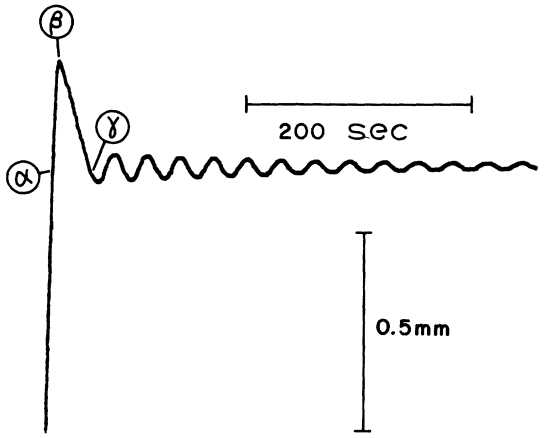

FIG. 7. Example of an anomalous initial oscillation peak. For this data the equilibrium level in reservoir A has been increased. Points α and γ indicate the first and second crossings of the new equilibrium level. At point β, reservoir A is being filled by film flow through the long flow path at the same rate it is being emptied by flow through the short flow path. For this particular data $T = 1.30$ K, $l_1/l_2 = \frac{1}{64}$ and $a_1/a_2 = 1$.

in use. Now imagine increasing the level of reservoir A in a series of steps, such that during each displacement the short flow path velocity goes critical. This can be accomplished for example by dropping the plunger in four successive equal steps. Because the long flow path is accelerated to a higher velocity after each step, one might expect to see both the net circulation and the anomalous first peak[42] also increase after each step. Such an event is recorded in Fig. 8, where it is clear that the first oscillation peak does indeed grow more anomalous while the subsequent oscillations grow smaller. The inset at the bottom shows the trapped circulation present at the beginning (A) and end (B) of the sequence as reflected by our heater S operation described in Sec. III B (see point 2 of Fig. 3 for reference). Circulation has been pumped into the system as a result of the steps in level. If the successive plunger steps are repeated starting from a different initial state of trapped circulation, the oscillations observed will display a different character. For example, compare Fig. 9 (in which the initial state consists of a large persistent current opposing the steps) to Fig. 8. The film flow resulting from the successive steps opposes the initial persistent current. Note that no anomalous peak is visible until the last displacement, and that the oscillation amplitudes tend to grow with each step. For the displacements where no anomalous peak is visible, one can relate $v_2(t_\alpha)$, the velocity in the long flow path at point α (see Fig. 7) to the oscillation amplitude $z_{\rm amp}$ by

$$\dot{z}(t_\alpha) \sim \omega z_{\rm amp} \sim a_1 v_c + a_2 v_2(t_\alpha)\,, \tag{17}$$

where the first and second relationships are consequences of the sinusoidal nature of the oscillations and mass continuity, respectively. If the initial v_2 is large and negative—the case for Fig. 9—the fluid in the long flow path will be *decelerated* during each run-in until $v_2 = 0$; from then on the displacements will *accelerate* v_2. As $v_2(t_\alpha)$ proceeds from a large negative value to a positive value one has from Eq. (17) that $z_{\rm amp}$ will increase as demonstrated in Fig. 9. Because there is dissipation during each of the plunger steps shown in Fig. 9 the circulation changes and the persistent current velocity is gradually reduced and accelerated in the step direction as shown.

Changes are much less dramatic for the case of an initial persistent current prepared such that v_2 is large and in the same sense as the displacements. For example, in Fig. 10 the initial persistence indicated in inset A is so large that at the end of the first displacement one can safely assume that $v_2(t_\alpha) = v_c$. The character of this first event is consequently the same as Fig. 7. Recall however,

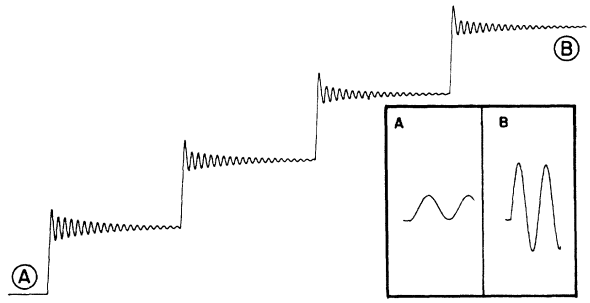

FIG. 8. Position of the free surface in reservoir A as a function of time. Starting from the state-of-zero persistent current (position A on the main trace) circulation is increased four times by successive plunger displacements. After the fourth displacement (B, main trace), the amount of trapped circulation can be documented by operation of the heater S (B, inset). For this figure, and for Figs. 9 and 10, each displacement corresponds to a 0.822-mm level change in reservoir A. The time interval between displacements is 620 sec, $T = 1.30$ K, $l_1/l_2 = \frac{1}{64}$, and $a_1/a_2 = 1$.

that v_2 is decelerated from α to γ so that if one were to sample for a persistent current just prior to the second displacement, one might find, dependent on the geometry and displacement size, a smaller magnitude circulation (see inset B, Fig. 10). For successive displacements the cycle will repeat as v_2 is accelerated to v_c during the run-in and decelerated from α to γ.

To more explicitly show the dependence of the peak structure $\alpha\beta\gamma$ (Fig. 7) on the magnitude and sense of a preexisting velocity v_2, we have prepared the film-flow loop[43] with persistent currents

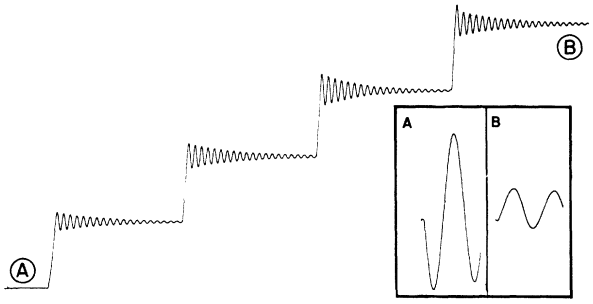

FIG. 9. Position of the free surface in reservoir A as a function of time. Inset A documents that the initial state (point A, main trace) is one in which a substantial persistent current preexists in a sense, so as to oppose the flow in the long flow path produced by the plunger motion. After the fourth plunger displacement, inset B shows that the level changes have reversed the sense of the persistent current. In this case the final persistent current has a smaller magnitude than the initial current. (See also Fig. 8 caption.)

of varying velocity and then reduced the level in reservoir A by a *small* distance to drive the short flow path critical (Fig. 11). Each event begins with an examination of the sense and magnitude of the persistent current in our apparatus, (closed configuration, Fig. 2), as evidenced by use of the heater S and ends with a sample of the persistent current left in the flow paths after the small change in level. To obtain these data we have used the heater located in the base of reservoir A. At the start of each trace in Fig. 11 the heater has been on (170 μW) for several minutes. The decrease in the level in each case is initiated by shutting off the heater. The thermal time constant of reservoir A (and also reservoir B) is about 25 msec, and of no consequence relative to the figures. The data are arranged such that the maximum persistent current opposing the level change is at the top of the figure. A gradual transition to zero circulation and then to maximum persistence reinforcing the level change is shown as one proceeds down the figure. Two important points are illustrated by the data in Fig. 11. First, because the level displacements are identical for all the events in the figure, the character of the oscillations can be correlated only with the persistent circulation already present in the flow loop prior to the displacement. Secondly, the drop time, that time interval from the initiation of the level displacement to the first zero crossing of the new equilibrium level, decreases as one proceeds down the figure. This is consistent with all of our previous analysis in that for large enough level displacements the fluid in the short flow path accelerates to v_c in a time short compared with the drop time regardless of the original flow direction in that path. Variations in the drop time then are primarily due to variations in the fluid velocity in

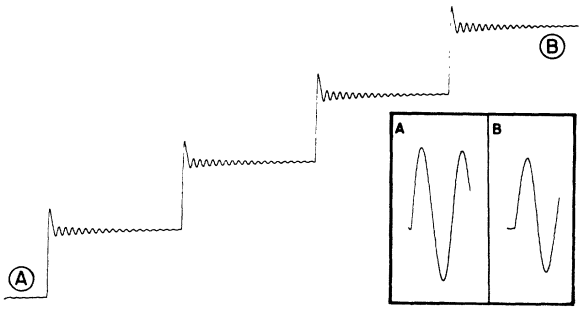

FIG. 10. Position of the free surface in reservoir A as a function of time. In this case the initial state is one in which a persistent current is present in the same sense as the flow in the long flow path induced by the motion of the plunger. The final persistent current is smaller than the initial persistent current. (See text and Fig. 8 caption.)

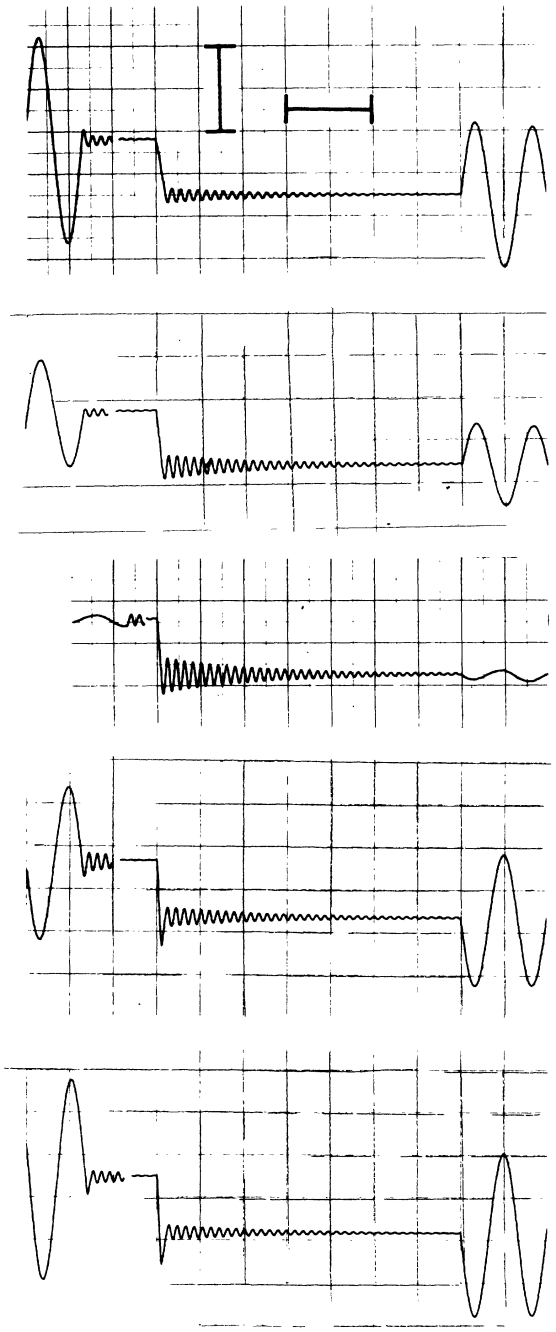

FIG. 11. Position of the free surface in reservoir A as a function of time for several level changes in the presence of various preexisting persistent currents. The magnitude and sense of the persistent current both before and after the small level change are shown in each case. The magnitude of the level change is (1) equal in each case and (2) small enough so as not to induce a significant persistent current on its own. For these data $T = 1.18$ K, $l = l_1/l_2 = \frac{1}{64}$, and $a = a_1/a_2 = 1$. The vertical bar represents a displacement of 250 μm in reservoir A and the horizontal bar represents an elapsed time of 200 sec.

the long flow path. If that velocity is large and in the same sense as the displacement, then a small acceleration toward the reservoir will result in a large mass flow into the reservoir and a shorter drop time. If instead the velocity is large, and in the opposite sense from the displacement, we expect that a small acceleration toward the reservoir will reduce only slightly the large mass flow out of the reservoir implied by the sense of v_2. This situation will then give rise to a longer drop time.

Figure 12 shows data similar to that in Fig. 11 from an experiment with a different geometry. While the qualitative behavior of the oscillations are the same for the two experiments, Fig. 12 shows generally larger oscillations relative to the step height and the anomalous peak height. We would expect such behavior when l_2 is reduced relative to l_1. Referring again to Fig. 7 it is clear that if the fluid in the long flow path, possessing less effective mass, is decelerated more quickly from α to γ then the emptying rate of the reservoir will be reduced. If this is so we would expect the fluid moving through the short flow path at v_c to regain point γ more quickly. Since less time is spent dissipating energy between β and γ the subsequent oscillations are larger in amplitude.

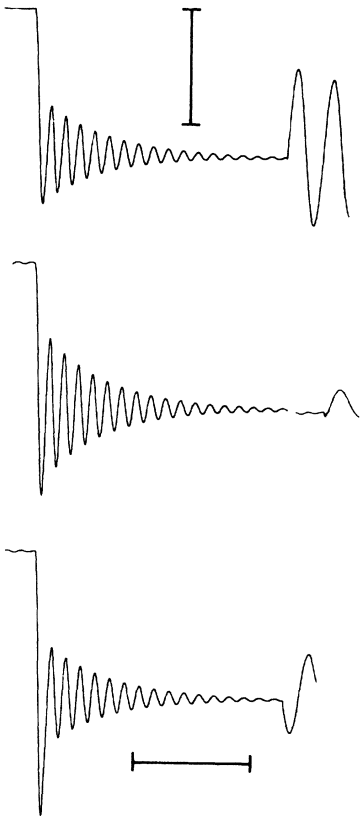

FIG. 12. Position of the free surface in reservoir A vs time at $T = 1.38$ K for $l = \frac{1}{20}$ and $a = 1$. As in Fig. 11, various persistent currents are present prior to the small change in level and the nature of the oscillation observed immediately following the level change depends on the preexisting current. The vertical bar represents a displacement of 150 μm, and the horizontal bar represents an elapsed time of 200 sec.

As Campbell[8] has pointed out, small level displacements can be used to test for the presence of circulation in a multiply connected geometry. Figure 13 illustrates how such a test may be made. The upper traces, I(a) and I(b), show the oscillations one observes following a small level change with no persistence built into the flow paths. The absence of any preexisting persistent current is documented by the observation that both oscillations I(a) and I(b) are symmetric, show no unusual first peak structure, and require equal times to reach point α. This is to be contrasted with what is observed in the pair of traces II(a) and II(b). In this case a substantial preexisting persistent current with a long flow-path flow toward reservoir A is indicated when the level in reservoir A is increased [II(a)] or decreased [II(b)]. In the pair of traces, III(a) and III(b), the opposite-sense persistent current must have been present prior to the changes in level. Although these methods

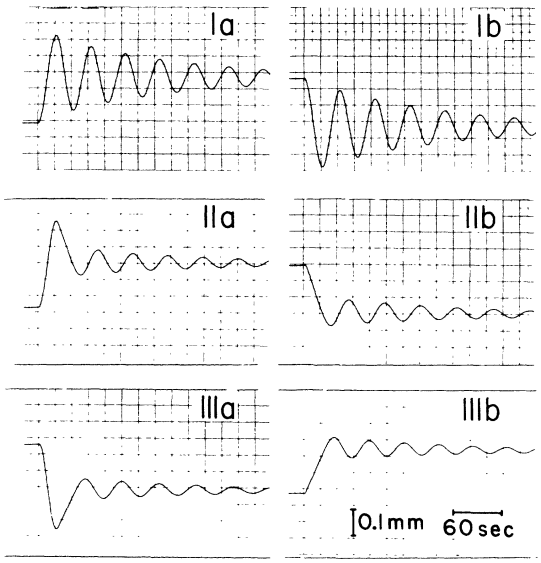

FIG. 13. Position of the free surface in reservoir A vs time showing how small displacements of the free surface equilibrium position may be used to reveal the existence of trapped circulation. The displacements are made in pairs; I(a) represents a fill and I(b) an empty for reservoir A. In I there is no preexisting circulation. In II circulation with long flow path flow toward reservoir A is present, while in III circulation of the opposite sense is present. Here we have used the plunger to initiate the slight level changes with $l = \frac{1}{64}$ and $a = 1$ at $T = 1.50$ K.

of probing the circulation are not very quantitative, they do serve as a means of verifying the the presence and sense of the circulation.

Campbell's theory[8] predicts that for small values of $l = l_1/l_2$ the shape of the first peak should be sensitive to changes in $a = a_1/a_2$ near 1. If we contrast Fig. 14 with Fig. 7 we see that this is indeed the case. Both figures are from data runs with $l \gg 1$ but for Fig. 7 we have (macroscopically $a = 1$, whereas in Fig. 14 $a = 0.85$. While the trace in Fig. 7 shows a sharp peak followed by an almost linear return to the equilibrium level, Fig. 14 exhibits a flattening of the peak resulting in a pronounced curvature from β to γ. This flattening can be understood from a consideration of the flow rates for the two paths: once $v_1 = v_c$, the changes in the net fill rate will be due primarily to changes in v_2, and these changes will be very gradual due to the large effective mass of the film in path l_2. In Fig. 7 this point takes place after β so that the peak sharpness is due to fill rate changes in both v_1 and v_2. If a_1 is reduced, thereby decreasing the maximum flow rate through the short flow path, it is possible that there could still be a net *fill* rate when $v_1 = v_c$ and $v_2 < v_c$ (point β' on Fig. 14). Thus the peak "sharpness" would be determined primarily by the rate of change of v_2 and in fact the peak would become flattened.

The evolution of this peak structure is documented in Fig. 15. Each event commences with zero trapped persistent current but with a relatively small-level oscillation (resulting from a previous heater operation having destroyed any circulation present in the flow loop). A calibration offset corresponding to a 2.16-mm level displacement is then recorded. The plunger is then stepped down, so as to increase the level and the measuring capacitor A fills to, and then oscillates about, the new equilibrium level. After these Atkins[6] oscillations—taking place primarily through the short flow path—have damped out, the gain is increased by a factor of 2.5 and the heater S is activated revealing the magnitude of any persistence trapped in the flow loop by the plunger-induced flow. Figure 15 shows a complete view of the evolution including the plunger-induced displacement and the resulting persistent current amplitude. One can define a critical drop height z_c which corresponds to the minimum displacement needed to drive both paths critical at the first zero crossing (i.e., point α in Fig. 7). This height is experimentally determined by realizing that the persistent current output (as determined by the operation of heater S) should saturate for displacements greater than or equal to z_c [Fig. 15(K)]. Similarly, the largest amplitude obtained for oscillations through l_2 should correspond to v_c and serve as a normalization point for the velocities obtained for our persistent current outputs. If one plots the normalized velocity as a function of the normalized drop height, Fig. 16 results. Perhaps the most interesting feature of Figs. 15 and 16 ($a = 0.85$) is that the large displacements ($z \gtrsim z_c$) do not produce the largest persistent currents. A clue to this behavior is provided by noting that the anomalous peak corresponding to the maximum persistent current (Fig. 15(I)) resembles Fig. 7 ($a = 1$) more than Fig. 14 ($a = 0.85$); the time from β to γ is relatively short. In effect, as the velocity v_2 at α increases, the peak $\alpha\beta$ gets larger which means that more time is required to proceed from β to γ. Since v_2 is decelerating from β to γ there comes a point where an increase in the velocity v_2 at α results in a net decrease at γ. This effect is predicted in the Campbell theory[8] and a calculation employing the approximations in Sec. IIB yields the solid curve in Fig. 16.

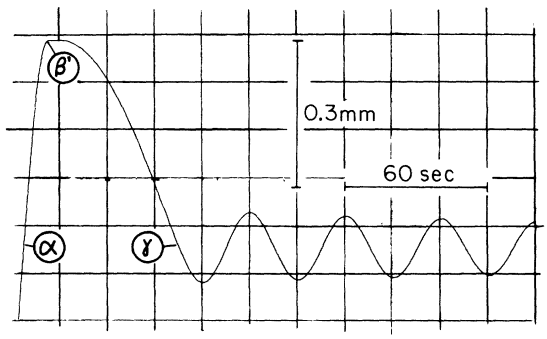

FIG. 14. Similar to Fig. 7 except here $l = \frac{1}{68}$ and $a = 0.85$. The peak is flattened at β' which results in curvature in the region from β' to γ. The difference between this figure and Fig. 7 is due primarily to the difference in the value of a. Here $T = 1.30$ K.

Figure 17 focuses specifically on the character of the initial peak. The sequence clearly illustrates that as the equilibrium level displacement (and so the velocity in the long flow path at α) increases, so must the anomalous peak height and the time from β to γ. At the same time the amplitude of the oscillations about the new equilibrium level tends to decrease. In Fig. 18 we plot the peak height (P) and the subsequent oscillation amplitude (A) versus the normalized displacement (z/z_c) for the data in Fig. 17. The predictions from the Campbell theory,[8] as indicated by the solid lines are in qualitative agreement with the data.

Note that for the intermediate displacements (Fig. 17), small-amplitude high-frequency oscillations[44,45] are superimposed on the Atkins[6] oscillations. These oscillations represent a third sound resonance[46] excited by the temperature and film

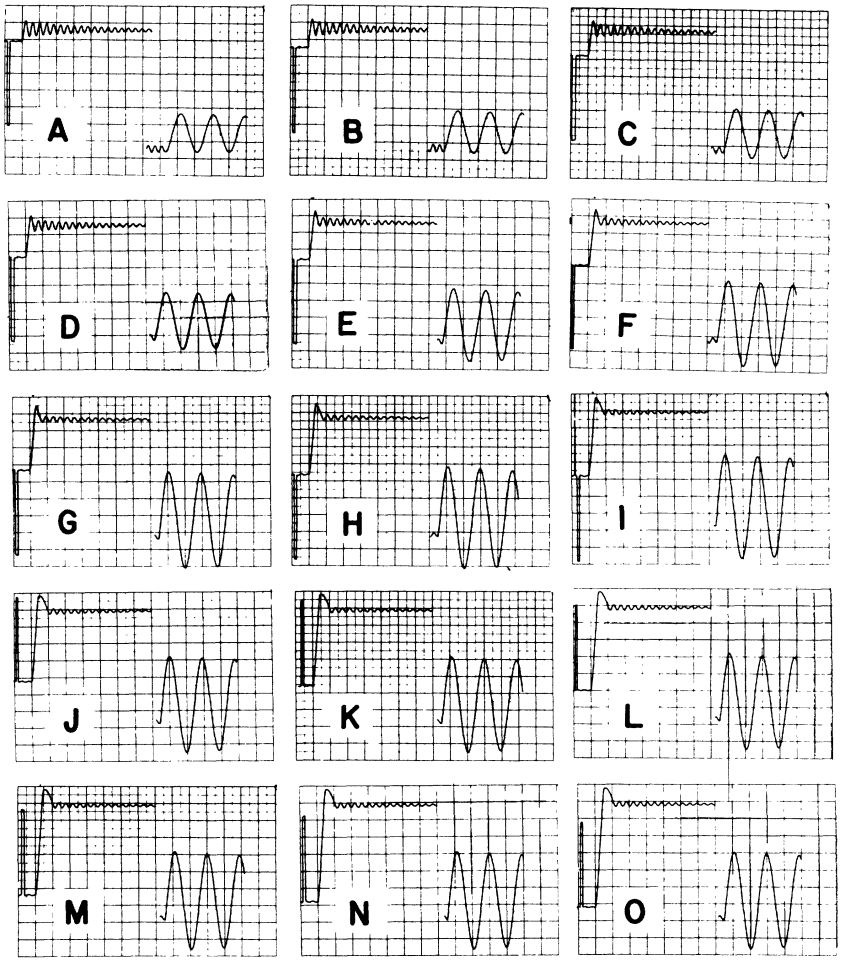

FIG. 15. Position of the free surface in reservoir A vs time for various size steps of the plunger. Each trace begins with no pre-existing trapped circulation and a calibration offset corresponding to a level change of 2.16 mm. At the conclusion of the Atkins oscillations following the motion of the plunger the magnitude and sense of the trapped circulation is documented by increasing the recorder gain by 2.5 and operation of the heater S. These data were obtained at $T = 1.30$ K for $l = \frac{1}{68}$ and $a = 0.85$. Each large horizontal division represents an elapsed time of 100 sec.

thickness perturbations induced by the plunger displacement. It is reasonable to expect that as the plunger displacement decreases, so must the accompanying perturbations and thus the third sound amplitude. On the other hand, since third sound oscillations may not be supported in a film moving at v_c, we would expect that displacements large enough to drive v_2 critical would not show this effect. That is, the drop for which the third sound oscillations disappeared [Fig. 17(K)] would correspond to z_c. Note that this argument yields a value for z_c consistent with the value determined previously [Fig. 15(K)] by persistent current saturation.

Some mention should be made here as to the reasons for the absence of a detailed quantitative comparison between the theory and our results. One reason is that in our apparatus damping is present. The introduction of damping into the equations in Sec. II B quickly leads to transcendental boundary equations, which in turn makes it much more difficult to make detailed predictions. Also, the dissipation approximation used in Sec. II B is not completely realistic in our apparatus. Previous data taken in this lab (see for instance Ref. 5, Fig. 6) and elsewhere indicate that the dissipation is a smooth function of velocity. We have not analyzed this dissipation well enough to fit parameters and a functional form $\vec{f}(\vec{v})$ for the present apparatus. Finally, and most importantly, we are reluctant to assign unique values to v_c, l_0, l_1, l_2, a_0, a_1, and a_2. There is no way in our apparatus that we can determine these seven quantities unambiguously. For instance, expressions for the frequency yield only the ratios a_j/l_j and conditions on critical flow rates yield products such as $a_j v_{j,c}$. Since we do not exactly know our film profile or our flow-path geometry (microscopic surface roughness[47] can greatly increase the effective perimeter and so the cross sectional film area), we have limited this discussion to a generally qualitative comparison.

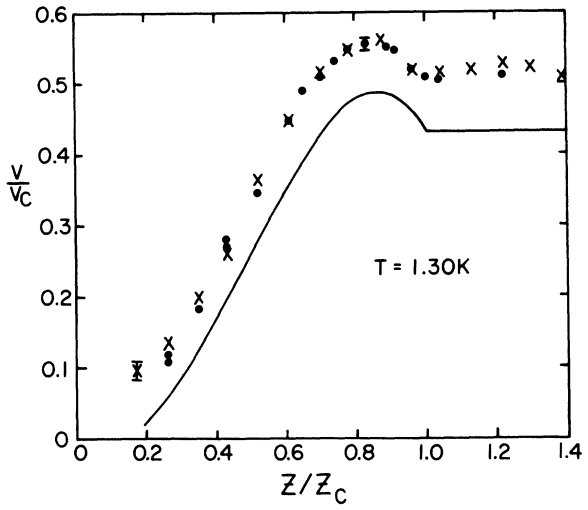

FIG. 16. Normalized persistent velocity resulting from a normalized change in the equilibrium level in reservoir *A* for the data of Fig. 15 (crosses) and for a similar series of data (dots) obtained in the same apparatus at a later time. The solid line represents the theoretical prediction based on the assumptions discussed in Sec. II B.

V. CONCLUSIONS

We have shown unambiguously that persistent circulation can be generated by superfluid film flow in a multiply connected two-reservoir system. The presence of the persistent circulation has been documented using previously developed techniques.[4] We have shown that the presence or generation of persistent circulation accompanying film flow has a characteristic effect[48] on the Atkins[6] oscillations of the superfluid levels in our reservoirs. These observations are in qualitative agreement with the predictions of Campbell.[8] Given the constraints imposed by both theoretical approximations and experimental uncertainties, the quantitative agreement is satisfactory. We have observed that the circulation in these saturated films is stable both in time and to the perturbation of an imposed film flow so long as the imposed flow does not result in an approach to the "critical velocity" on the flow paths (see Appendix A).

ACKNOWLEDGMENTS

We would like to thank K. L. Telschow for many helpful suggestions and discussions. We are also indebted to L. J. Campbell for several helpful comments and an enthusiastic interest in our work.

APPENDIX A

In anticipation of subsequent measurements of persistent currents in unsaturated films,[49] other experiments were undertaken to investigate the conditions for creation and conservation of circulation. A prediction of Eq. (3) is that for subcritical velocities [such that $\tilde{f}(\tilde{v})$ is immeasurably small] the circulation should be conserved on the flow loop. This prediction was examined in our apparatus (Fig. 2) in the following manner. First, any preexisting circulation in the loop was eliminated by operation of the heater *S*. Then the voltage was gradually increased (see inset Fig. 19) to the heater in reservoir *A* and subsequently de-

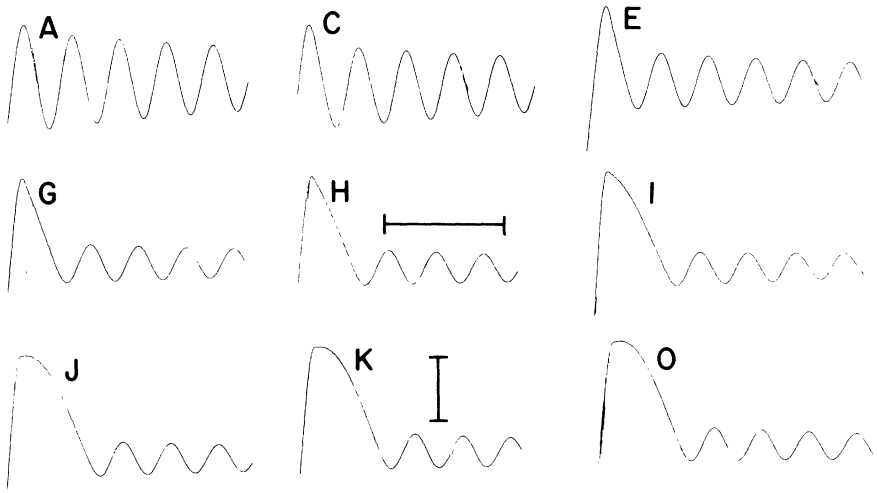

FIG. 17. Detailed examination of the evolution of the oscillations obtained in the manner represented in Fig. 15. The vertical bar represents a displacement of 282 μm and the horizontal bar represents an elapsed time of 100 sec. Note the presence of third sound on recordings I and J. The third sound is visible but less obvious on G and H. The letters identifying the various recordings can be compared to those used in Fig. 15. Although these recordings are distinct from those of Fig. 15 the same magnitude level displacements were used in corresponding cases.

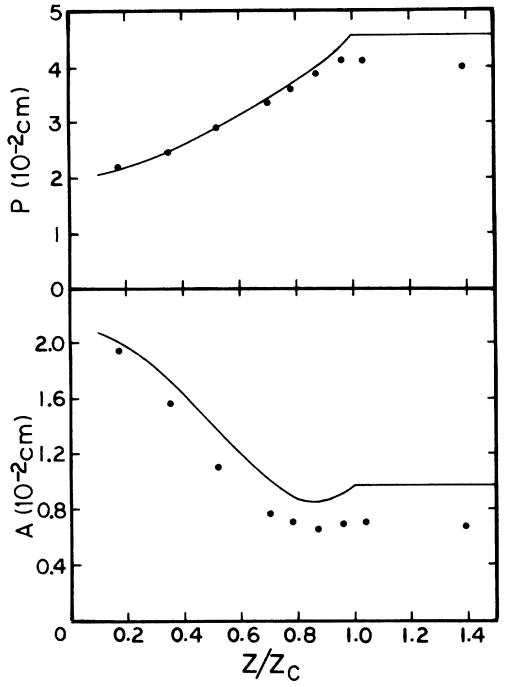

FIG. 18. (a) First oscillation peak height P vs the normalized level change in reservoir A, z/z_c. (b) Subsequent Atkins oscillation amplitude A (corrected for Robinson damping) vs z/z_c. Both (a) and (b) are for the data of Fig. 17. The solid lines in both cases represent predictions of theory based on the approximations discussed in Sec. IIB. The measurement errors are smaller than the size of the symbols.

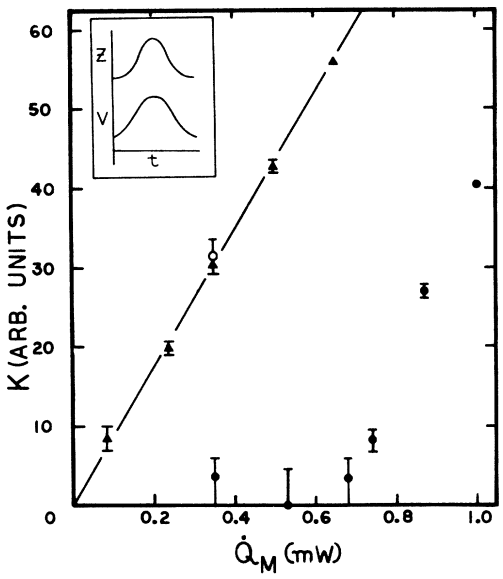

FIG. 19. Circulation (measured by the heater operation) as a function of reservoir heater power. The inset indicates how the voltage is applied to the heater and how the reservoir level consequently rises. The error bars are deduced from a constant estimated amplitude measuring error applied to Eq. (16). The various symbols are discussed in detail in the text.

creased to zero. The heat generated in reservoir A caused both a rise in the level of the reservoir and, importantly, a flow of superfluid through the two flow paths toward the reservoir to replace atoms lost from the reservoir due to evaporation. Under these quasistatic conditions the velocity in the flow paths was expected to have been directly related to the given voltage and no dissipation resulted from rapid accelerations in the flow paths. After the detector heater voltage was returned to zero the flow path heater S was operated in the previously described manner to test for persistent circulation. The magnitude of the resulting persistent current was then measured as a function of the maximum power to the reservoir A heater, $\dot{Q}_M$. The results of this operation for various maximum applied heater powers are represented by solid circles in Fig. 19. For maximum heater powers $\dot{Q}_M$ *below some nominal threshold* the circulation at the end of the above procedure is observed to be unchanged, i.e., zero. That is,

$$K = v_2 l_2 - v_1 l_1 = 0 , \tag{18}$$

as predicted by Eq. (3) independent of the detector heater power. Above the heater threshold, $v_1 = v_c$ and dissipation occurs but v_2 is still free to increase with the applied power, so that we observe a nonzero final circulation

$$K = v_2 l_2 - v_c l_1 \propto \dot{Q}_M - \text{const} . \tag{19}$$

Nonzero final circulation could also be created in the region where $v_1 < v_c$ by simply pulsing heater S *once* at the point of maximum heater power. Immediately prior to the heat pulse to S one expects that

$$K = 0 = v_2 l_2 - v_1 l_1 \Rightarrow v_1 = v_2 / l \tag{20}$$

and

$$\dot{Q}_M \propto a_2 v_2 + a_1 v_1 = a_2 v_2 (1 + a/l) , \tag{21}$$

where once again $a = a_1/a_2$ and $l = l_1/l_2$. The pulse to heater S temporarily blocks the short flow path so that immediately after the pulse one expects $v_1' = 0$ and

$$\dot{Q}_M \propto a_2 v_2' = a_2 v_2 (1 + a/l) , \tag{22}$$

$$K' = v_2' l_2 = v_2 l_2 (1 + a/l) . \tag{23}$$

If the power to the heater in reservoir A is then reduced to zero, the circulation K' should persist in the flow loop and be detected by the activation of heater S in the usual manner. The result of

this procedure for one $\dot{Q}_M$ is indicated in Fig. 19 by the open circle.

A somewhat different but equivalent way of performing this same measurement was to instantaneously apply $\dot{Q}_M$ to the detector heater and then to wait a short while for the reservoir levels to adjust to the new equilibrium values. Heater S was then operated in the manner demonstrated in Fig. 3, event 4–5, to eliminate any *apparent* circulation present in the flow loop. Because a bias current still flows through the long flow path as heater S is deactivated (such that $\dot{z}=0$) and $v_1=0$, one would expect to obtain Eqs. (22)and (23) again. After a reduction of the detector heater power to zero, one should then find a nonzero circulation that should be consistent with the open circle in Fig. 19 and have the predicted dependence of $K \propto \dot{Q}_M$. In fact such a dependence is exhibited by the data as shown by the solid triangles in Fig. 19. The data further support the conclusion that circulation is conserved in our apparatus in the absence of applied dissipation.

---

*Supported by the NSF Grant Nos. DMR72-03138 and DMR76-08260.

†Work supported in part by the Alfred P. Sloan Foundation.

[1]W. F. Vinen, Proc. R. Soc. Lond. A 260, 218 (1961).

[2]R. P. Henkel, G. Kukich, and J. D. Reppy, in *Proceedings of the Eleventh International Conference on Low Temperature Physics*, edited by J. F. Allen, D. M. Finlayson, and D. M. McCall (St. Andrews, Scotland, 1968), Vol. 1, p. 178.

[3]F. Wagner, J. Low Temp. Phys. 13, 185 (1973).

[4]R. K. Galkiewicz and R. B. Hallock, Phys. Rev. Lett. 33, 1073 (1974).

[5]R. B. Hallock and E. B. Flint, Phys. Rev. A 10, 1285 (1974).

[6]K. R. Atkins, Proc. R. Soc. Lond. A 203, 119 (1950).

[7]J. F. Robinson, Phys. Rev. 82, 440 (1951).

[8]L. J. Campbell, Physica (Utr.) 78, 245 (1974).

[9]L. J. Campbell, in *The Helium Liquids*, edited by J. F. Allen and J. G. M. Armitage (Plenum, New York, 1975).

[10]E. F. Hammel, W. E. Keller, and R. H. Sherman, Phys. Rev. Lett. 24, 712 (1970).

[11]E. B. Flint, Ph.D. thesis (University of Massachusetts, 1974) (unpublished).

[12]M. E. Banton (private communication).

[13]See also, S. C. Whitmore and W. Zimmerman, Phys. Rev. Lett. 15, 391 (1965).

[14]P. J. Bendt, Phys. Rev. 127, 1441 (1962).

[15]D. Depatie, J. D. Reppy, and C. T. Lane, in *Proceedings of the Eighth International Conference on Low Temperature Physics*, edited by R. O. Davies (Butterworths, London, 1962), p. 75.

[16]J. D. Reppy and D. Depatie, Phys. Rev. Lett. 12, 187 (1964).

[17]J. D. Reppy, Phys. Rev. Lett. 14, 733 (1965).

[18]J. B. Mehl and W. Zimmerman, Jr., Phys. Rev. Lett. 14, 815 (1965).

[19]J. R. Clow and J. D. Reppy, Phys. Rev. Lett. 16, 887 (1966).

[20]J. R. Clow and J. D. Reppy, Phys. Rev. Lett. 19, 291 (1967).

[21]G. Kukich, R. P. Henkel, and J. D. Reppy, Phys. Rev. Lett. 21, 197 (1968).

[22]W. M. van Alphen, R. De Bruyn Ouboter, K. W. Taconis, and E. Van Spronsen, Physica (Utr.) 39, 109 (1968).

[23]P. Sikora, E. F. Hammel, and W. E. Keller, Physica (Utr.) 32, 1693 (1966).

[24]H. Kojima, W. Veith, S. J. Putterman, E. Guyon, and I. Rudnick, Phys. Rev. Lett. 27, 714 (1971).

[25]H. W. Chan, A. W. Yanof, F. D. M. Pobell, and J. D. Reppy, in *Proceedings of the Thirteenth International Conference on Low Temperature Physics*, edited by K. D. Timmerhaus, W. J. O'Sullivan, and E. F. Hammel (Plenum, New York, 1974), Vol. 1, p.229.

[26]R. P. Henkel, E. N. Smith, and J. D. Reppy, Phys. Rev. Lett. 23, 1276 (1969).

[27]T. G. Wang and I. Rudnick in Ref. 25, p. 239.

[28]H. J. Verbeek, E. van Spronsen, H. Mars, H. van Beelan, R. de Bruyn Ouboter, and K. W. Taconis, Physica (Utr.) 73, 621 (1974).

[29]E. van Spronsen, H. J. Verbeek, R. de Bruyn Ouboter, K. W. Taconis, and H. van Beelan, Physica (Utr.) 77, 131 (1974).

[30]G. A. Williams and R. E. Packard, Phys. Rev. Lett. 32, 587 (1974) [see also R. B. Hallock, Phys. Lett. A 51, 457 (1975); and L. J. Campbell, Phys. Rev. B 11, 4721 (1975)].

[31]J. K. Hoffer, J. C. Fraser, E. F. Hammel, L. J. Campbell, W. E. Keller, and R. H. Sherman in Ref. 25, p. 253. [See also, L. J. Campbell, E. F. Hammel, J. K. Hoffer, and W. E. Keller, J. Low Temp. Phys. 24, 527 (1976)].

[32]J. F. Allen, J. G. M. Armitage, and B. L. Saunders in Ref. 25, p. 31.

[33]J. F. Allen, in *Proceedings of the International School of Physics, Course No. XXI-Liquid Helium*, edited by G. Careri (Academic, New York, 1963), p. 305.

[34]P. Calvoni, R. Greulich, and B. Maraviglia, Nuovo Cimento Lett. 6, 536 (1973).

[35]J. S. Langer and J. D. Reppy, in *Progress in Low Temperature Physics*, edited by C. J. Gorter (North-Holland, Amsterdam, 1970), Vol. 6, p. 1.

[36]R. B. Hallock and E. B. Flint, Phys. Rev. Lett. 31, 1383 (1973).

[37]F. London, *Superfluids* (Dover, New York, 1954), Vol. II, p. 70.

[38]R. J. Donnelly and P. H. Roberts, Philos. Trans. R. Soc. Lond. 271, 41 (1971).

[39]Millipore Filter, Millipore Corp., Bedford, Mass.

[40]R. B. Hallock, Rev. Sci. Instrum. 43, 1713 (1972).

[41]The persistent current experiments reported in Ref. 28 saw no detectable change for times as long as 18 h.

[42]M. E. Banton has also seen experimental evidence for this (private communication from L. J. Campbell).

[43]Since the flow paths are approximately the same height above the free surface, we make the operational definition of $a = a_1/a_2$ as the ratio of the smallest macroscopic radius of the short flow path to the smallest macroscopic radius of the long flow path. The lengths are then as defined following Eq. (4).

[44]R. K. Galkiewicz, K. L. Telschow, and R. B. Hallock, *Proceedings of the Fourteenth Conference on Low Temperature Physics*, edited by M. Krusius and M. Vuorio (North-Holland, Amsterdam, 1975), Vol. 1, p. 415.

[45]K. L. Telschow, R. K. Galkiewicz, and R. B. Hallock, Phys. Rev. B 14, 4883 (1976).

[46]Third sound has previously been observed as a perturbation of Atkins (Ref. 6) oscillations by E. van Spronsen, H. J. Verbeek, H. van Beelan, R. de Bruyn Ouboter, and K. W. Taconis, Physica (Utr.) 77, 570 (1974).

[47]R. K. Galkiewicz, K. L. Telschow, and R. B. Hallock, J. Low Temp. Phys. 26, 147 (1977).

[48]A preliminary report based on very limited data has appeared previously: R. K. Galkiewicz and R. B. Hallock, in Ref. 44, p. 407.

[49]K. L. Telschow and R. B. Hallock, Phys. Rev. Lett. 37, 1484 (1976).